Alternative stable river bed states at high flow

S.I. de Lange[1], R.C. van de Vijsel[1], P.J.J.F. Torfs[2], A.J.F. Hoitink[1]

[1]Wageningen University, Department of Environmental Sciences, Hydrology and Quantitative Water Management, Wageningen, the Netherlands
[2]Independent researcher

Key Points:

- River dunes exhibit bimodal height distributions at high transport stages, caused by rapid shifts between dunes and Upper Stage Plane Bed.
- This can be interpreted as tipping behavior, i.e. flickering between two stable states.
- Tipping behavior in geomorphology calls for experimental designs with replication and reinterpretation of classical equilibrium relations.

Corresponding author: Sjoukje de Lange, sjoukje.delange@wur.nl

Abstract

River bedforms influence fluvial hydraulics by altering bed roughness. With increasing flow velocity, subaqueous bedforms transition from flat beds to ripples, dunes, and an Upper Stage Plane Bed. Although prior research notes increased bedform height variation with flow strength and rapid shifts between bed configurations, the latter remains understudied. This study reanalyzes data from earlier experiments, and reveals a bimodal distribution of dune heights emerges beyond a transport stage of 18. Dune heights flicker between a low and high alternative state, indicating critical transitions. Potentially triggered by local sediment outbursts, these shifts lead to dune formation before returning to an Upper Stage Plane Bed. This flickering behavior challenges the adequacy of a single snapshot to capture the system's state, impacting field measurements and experimental designs, and questions the classical equilibrium equations. This study calls for further research to understand and quantify flickering behavior in sediment beds at high transport stages.

Plain Language Summary

As the flow velocity of a river increases, the riverbed changes from being flat to having ripples, which develop into larger dunes and flat bed conditions. At high flow velocities, these observed bedforms become more variable, and bedforms can alternate between different shapes in a short time. Surprisingly, not much attention has been paid to understanding how these dunes behave when the river flows increase, which is crucial for predicting floods. This study re-examines data from previous experiments to better understand ambiguity in the relation. We found that as the flow increases, the riverbed does not settle into one stable bedform state, but instead keeps switching between two forms. This behavior can be attributed to flickering, which are repeated critical transitions between alternative stable states. This flickering behavior has large implications for how we measure rivers in the field and design experiments in the laboratory. The study suggests there is a need for more research to consider ambiguous relations in geomorphology.

1 Introduction

Subaqueous river bedforms are ubiquitous in low-land rivers, and they are known to impact the river by altering its hydraulics, ecology, and sediment balance. In this way, the geometry of river bedforms impacts the fairway depth (ASCE Task Force, 2002; Best, 2005) and impacts dredging requirements, they add to the form roughness of the river bed (Warmink et al., 2013; Venditti and Bradley, 2022) impacting the water level, and determine suitable foraging places for fish (Greene et al., 2020). In the lower flow regime (Froude number lower than one), and for a given grain size, various types of river bedforms can form, depending on the strength of the flow (e.g. Gilbert, 1914; Guy et al., 1966). Below the threshold of sediment motion, the river bed can be flat, but as the flow increases, a continuum of bedforms evolves, consisting of ripples, followed by dunes, and eventually the dunes may wash out to an Upper Stage Plane Bed. This sequence is generally summarized in phase diagrams (Berg and Gelder, 1993; Southard and Boguchwal, 1990) which correlate a measure of flow strength and a measure of grain size to various bedform planforms.

The height of the dunes, which increases with increasing flow strength and subsequently decays into Upper Stage Plane Bed, can be estimated using bedform predictors. For this purpose, Venditti and Bradley (2022) developed empirical equations for dune height prediction based on transport stage T, which is a measure of relative flow strength. T is defined as the ratio of the Shields stress θ and the critical Shields stress θ_c. The empirical equation for dune height Δ (m) as described below is obtained from laboratory studies (i.e. flows with a water depth h less than 0.25 m), and yields a parabolic relation between dune height Δ and transport stage T:

$$\frac{\Delta}{h} = -0.00100 \left(\frac{\theta}{\theta_c} - 17.7 \right)^2 + 0.417 \tag{1}$$

Large scatter was observed when comparing the results from bedform height predictors to actual measurements (Bradley and Venditti, 2017), and various researchers describe an increased variability in bed geometry with increasing transport stage (Venditti et al., 2016; Bradley and Venditti, 2019; Saunderson and Lockett, 1983) (Figure 1). The large variability at high transport stages might be the reason that not many measurements and lab experiments are done in the regime where dunes transition into a flat bed (Karim, 1995). Despite the importance of dune behavior at high flow stages for, e.g., flood prediction (Julien and Klaassen, 1995) and infrastructure stability (Amsler and Schreider, 1999; Amsler and Garcia, 1997), not much attention has been given to this phenomenon.

The increased variability in bedform height with increasing transport stage is visualized using the data of Venditti et al. (2016) and Bradley and Venditti (2019) in Figure 1. Bradley and Venditti (2019) stated a "tremendous variability" between bed states at a higher transport stage, and reasoned that numerous observations of the bed are needed to get an average bed state that actually scales with transport state. Saunderson and Lockett (1983) did experiments around the transition from dunes to plane bed. They found four different bed states (asymmetrical dunes, convex dunes, humpback dunes, and flat bed) that the bed alternated between. They attributed this behavior to the close position of the system to a bed-phase boundary (from dunes to USPB). Venditti et al. (2016) more thoroughly explored the variability at large transport stages, and they grouped the resulting geometries into three phases: a plane bed with washed-out dunes, a field of large dunes, and a field of small dunes. They observed that the transition between these phases was continuous, and that water depth, shear stress and water surface slope co-varied with bed state. During plane bed conditions, intense erosion on the flat areas lead to localized incision, followed by the formation of small or large bedforms, which in turn washed out into a flat bed. The time they observed between the phases varied between minutes to more than half an hour, with transitions between the phases happening in seconds or minutes.

Despite this phenomenon being observed for multiple decades, it has received little attention, and an explanation for the increase in variability in bedform geometry with increasing transport stage is lacking. In this study, we suggest a possible explanation for this behavior, based on the theory of critical transitions (Scheffer et al., 2009; Scheffer et al., 2012; Lenton, 2013; Strogatz, 2018). This framework describes how sudden shifts to a qualitatively different (stable) regime can occur, once a system exceeds a critical bifurcation or tipping point. We hypothesise that in the transition from the dune regime towards Upper Stage Plane Bed, the bed exhibits flickering behavior (Dakos et al., 2013), resulting from repeated state shifts between alternative stable states due to stochastic perturbations. To support this hypothesis, we reanalyze the data from Bradley and Venditti (2019) and Venditti et al. (2016) and show how the results seamlessly fit in the critical transition framework.

2 Methods

2.1 Temporal data of bed morphology

To test our hypothesis, we reanalyze the temporal bedform data obtained in Venditti et al. (2016) and Bradley and Venditti (2019), which are visualized in Figure 1. The experiments from both studies were executed in the River Dynamics Laboratory at Simon Fraser University, Canada. Their flume has an adjustable flow, recirculates water and sediment, and is 15 m long (12 m working section), 1 m wide and maximum 0.6 m deep. In both studies, the experiments were performed with unimodal sediment with a D_{50} of 550 μm.

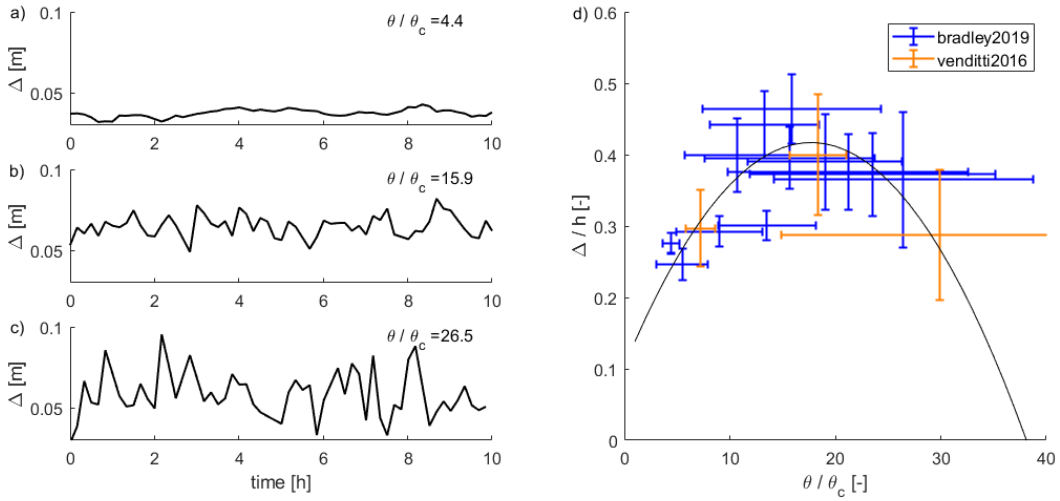

Figure 1. a-c) Dune height Δ over time for three experiments of Bradley and Venditti (2019), for three different transport stages θ/θ_c (i.e., bed shear stress divided by critical shear stress). d) Variability in non-dimensional dune height Δ/h increases with transport stage. Here, h is time-averaged water depth. The predictive equation of Venditti and Bradley (2022) (equation 1) is shown in black. Colored error bars indicate standard deviation for the experiments of Venditti et al. (2016) (red) and Bradley and Venditti (2019) (blue).

Venditti et al. (2016) conducted three experimental runs, under bed load, mixed load and suspended load-dominated conditions, resulting in mean flow velocities of 0.43, 0.59 and 0.87 m s^{-1} with corresponding observed transport stages of 7.12, 18.3 and 29.7. These suspended load-dominated conditions were at the threshold of washing out. The bathymetry was measured every 10 minutes for the bed load and mixed load conditions, and every 5 minutes for the suspended load-dominated experiments. Measurements started after the bed already had fully adjusted to the flow.

Bradley and Venditti (2019) broadened the scope of these experiments by performing 15 experiments under five different transport conditions: threshold of motion, bed load, lower mixed load, upper mixed load, and suspended load-dominated conditions. Additionally, they varied the water depth in three steps between 15 and 25 cm, although for the highest water depth they only performed threshold and bed load-dominated experiments due to the capacity of the flume. These conditions resulted in a mean velocity of 0.43 and 1.1 m s^{-1}, and resulting mean transport stages between 4.4 and 26.45. They scanned the bed every 10 minutes, but only after the bed had fully adjusted to flow.

2.2 Theoretical framework: critical transitions

The unstable behavior close to the bed-phase boundary can be interpreted using the framework of critical transitions (Scheffer et al., 2009). A critical transition is a regime shift where a system shifts rapidly to a qualitatively different state or dynamical regime, once a critical threshold (a critical bifurcation or tipping point) is exceeded (Scheffer et al., 2009; Lenton, 2013). The framework of critical transitions has been successfully employed to interpret observations of large and rapid shifts, amongst others in ecology, climate dynamics, medicine and finance Scheffer et al., 2012; Lenton, 2013, whereas it has found relatively little consideration in geomorphology (Hoitink et al., 2020). Many different types of tipping points exist, each described by different mathematical equations (Strogatz, 2018). Here, we focus

on the so-called supercritical pitchfork bifurcation, as we hypothesize that this model system could explain the observed increase in bedform variability towards higher transport stages (Figure 1).

The simplest model that generates a supercritical pitchfork bifurcation is given by the following differential equation:

$$\frac{dy}{dt} = ry - y^3 \tag{2}$$

with state variable y, control parameter r and time t. For $r < 0$, this differential equation has one equilibrium solution (i.e., where $dy/dt = 0$), namely $\bar{y} = 0$. This equilibrium is stable to small perturbations (Strogatz, 2018), meaning that perturbations dampen out and the system returns to equilibrium. For $r > 0$, the solution $\bar{y} = 0$ becomes unstable, meaning that small perturbations amplify and the system moves away from its equilibrium when perturbed. For $r > 0$, two other stable solutions emerge, $\bar{y} = \pm\sqrt{r}$. When visualized in a stability diagram, which shows how equilibrium state $\bar{y}$ varies with r, this behavior resembles a pitchfork; hence the name.

The increased variance with increasing transport stage (Figure 1d) can be explained by the emergence of a second equilibrium state, resembling the behavior in a supercritical pitchfork bifurcation. However, instead of a "central" equilibrium solution that is independent of control parameter r, i.e. $\bar{y} = 0$, we expect this central equilibrium to be a parabola, similar to the dune height predictor (equation 1). We therefore substitute $y = -a + br^2 + x$ in equation 2, with constants a and b and state variable x. Assuming that changes in r are much slower than changes in x, we can write $dy/dt = dx/dt$, and equation 2 becomes

$$\frac{dx}{dt} = r(-a + br^2 + x) - (-a + br^2 + x)^3 \tag{3}$$

Instead of the constant equilibrium $\bar{y} = 0$, the "central" solution of this modified pitchfork bifurcation now becomes a parabola, i.e. $\bar{x} = a - br^2$, which again is stable for $r < 0$ and unstable for $r > 0$. For $r > 0$, the two newly emerging solutions, $\bar{x} = a - br^2 \pm \sqrt{r}$, are stable. These equilibria are shown in Figure 2, with stable equilibria indicated in solid black lines, the unstable equilibrium as a dashed black line, and the bifurcation point ($r = 0$) as a black circle.

We hypothesize that the rapid shifts between high and low dune height observed at high transport stages (Figure 1c) are an expression of flickering. Flickering is a phenomenon described within the framework of critical transitions as a back-and-forth tipping between alternative stable states due to stochastic perturbations (Horsthemke and Lefever, 1984; Scheffer et al., 2012; Dakos et al., 2013). Indicators for flickering are multi-modality and a high variance (Scheffer et al., 2012; Dakos et al., 2012; Carpenter and Brock, 2006). As long as a system only has one stable equilibrium ($r < 0$ in Figure 2a), observation time-series of system state will show a unimodal frequency distribution spread around the theoretical equilibrium solution (Figure 2b). However, once a second equilibrium solution emerges ($r > 0$ in Figure 2a), the stochastic perturbations will occasionally cause the system to tip from one stable state into the other, which is reflected in a bimodally distributed system state (Figure 2d-f).

To illustrate flickering in the case of the modified pitchfork bifurcation, we generated a synthetic time series by numerically solving equation 3 while imposing continuous stochastic perturbations in x. We gradually vary control parameter r over time, i.e. $r(t) = r(0) + \frac{dr}{dt}t$, with $\frac{dr}{dt}$ a fixed rate of change. We numerically discretize equation 3 over time using a 4th-order Runge-Kutta scheme (Strogatz, 2018). Writing

$$\frac{dx}{dt} = f(x, t) \tag{4}$$

we then time-integrate the differential equation by calculating subsequent steps

$$dx = f(x, t)dt + dW(0, \sigma_W) \tag{5}$$

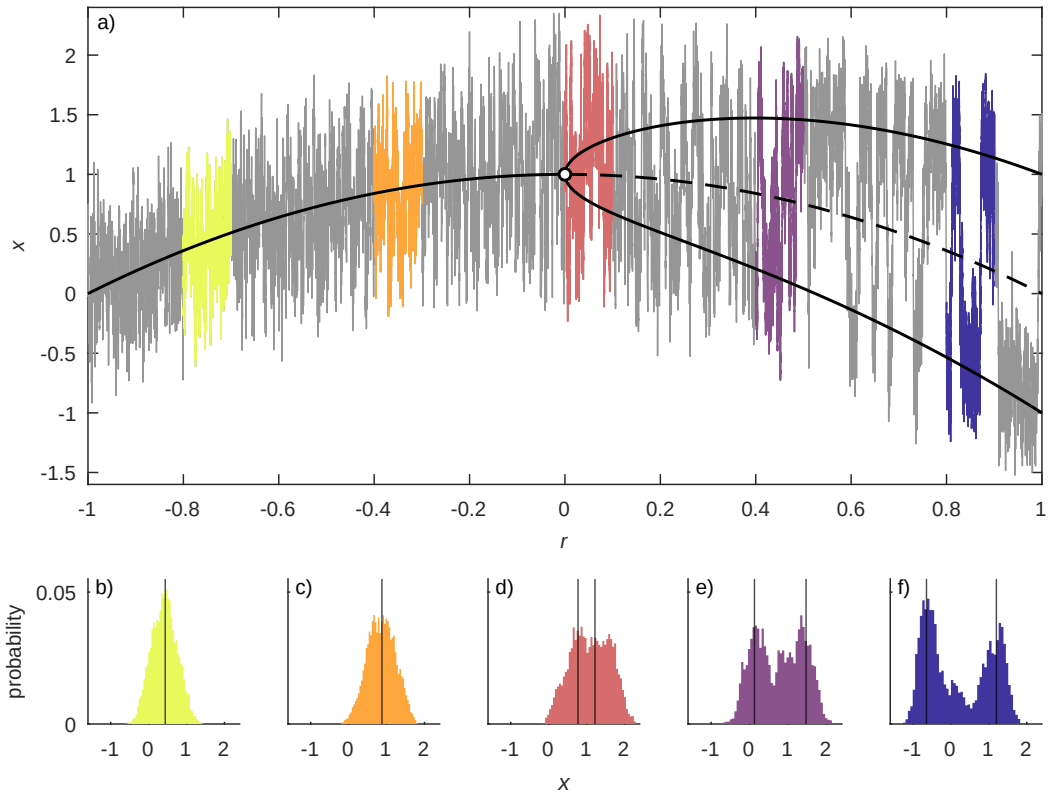

Figure 2. Model-generated flickering around a modified pitchfork bifurcation, i.e. the equilibrium solutions of equation 3. Solid black lines indicate stable equilibria, dashed black line indicates an unstable equilibrium, and the black circle indicates the pitchfork bifurcation point. Grey lines are simulated time series, i.e. the solution of the differential equation, with white noise added. Histograms of five time intervals are shown in corresponding colors below. Vertical black lines indicate the location of the stable equilibrium solution(s).

where $dW(0, \sigma_W)$ is a white noise signal, i.e. a random number drawn at each time step dt from a Gaussian distribution with mean 0 and standard deviation σ_W. In our case, $r(0) = -1$, $dr/dt = 0.001$, $dt = 0.01$, $a = 1$, $b = 1$ and $\sigma_W = 0.05$. This simple model demonstrates how flickering around the only existing equilibrium state $\bar{x} = a - br^2$ for $r < 0$ results in a unimodal frequency distribution of x, and a bimodal frequency distribution for $r > 0$, with the modes corresponding to the two emerging stable solutions $\bar{x} = a - br^2 \pm \sqrt{r}$.

2.3 Statistical analysis

To quantify variability in dune height, the standard deviation (σ) is determined as:

$$\sigma = \sqrt{\frac{\sum_{i=1}^{N} |x_i - \mu|^2}{N}} \tag{6}$$

in which x_i are the observations, μ is the mean of the data set, and N is the number of data points in the population.

To determine if a dune height distribution is bimodal, and to locate the modi of the distribution, a method based on Laplace's demon is used (Statisticat, 2021). This is a deterministic function that uses the kernel density of the dataset and reports a number of modes equal to half the number of changes in direction (i.e. where it switches from going up to going down). The function does not report modi that cover less than 10% of the distributional area.

If the distribution is indeed bimodal, the bimodality is considered significant if the distance between the two modi d_{modi} is larger than the coefficient of variation CV (i.e. the normalized standard deviation):

$$CV = \frac{\sigma}{\mu} \tag{7}$$

3 Results and Discussion

3.1 Increasing variability of bedform height with transport stage

The raw data as shown in Figure 1 indirectly identify the increase of variability in dune height with transport stage. When this variability is expressed in the standard deviation σ (equation 6), a significant linear relation ($\mathrm{R}^2 = 0.67$) between transport stage and standard deviation in non-dimensional dune height (Figure 3a) is revealed. Clearly, dune height becomes more variable with increasing flow strength.

From the 15 experiments analyzed, nine of them were characterized by a bimodal distribution (Supplementary Materials Figure S1). The distance between the identified modi, d_{modi}, increases with an increasing transport stage (Figure 3b), featuring a significant linear relation ($\mathrm{R}^2 = 0.74$). The modality of the distributions becomes significant if the distance between the modi is larger than the coefficient of variation, which is true for all experiments with a transport stage higher than 18. This behavior is comparable to the increase in d_{modi} as result of a pitchfork bifurcation (Figure 2).

3.2 Emergence of a second bedform state

The observed increase in bed height variability with increasing transport stages can be interpreted as the emergence of a second equilibrium branch. This becomes apparent when visualizing the raw data from Figure 1 in a two-dimensional histogram or density plot (Figure 4). For $\theta/\theta_c < 18$, the dune height observations are distributed in a relatively narrow zone around the theoretical dune height predictor (equation 1). The fitted modal distributions are either unimodal, or bimodal but with non-significant bimodality. For $\theta/\theta_c > 18$, the observations fan out towards higher and lower values of Δ/h. For three

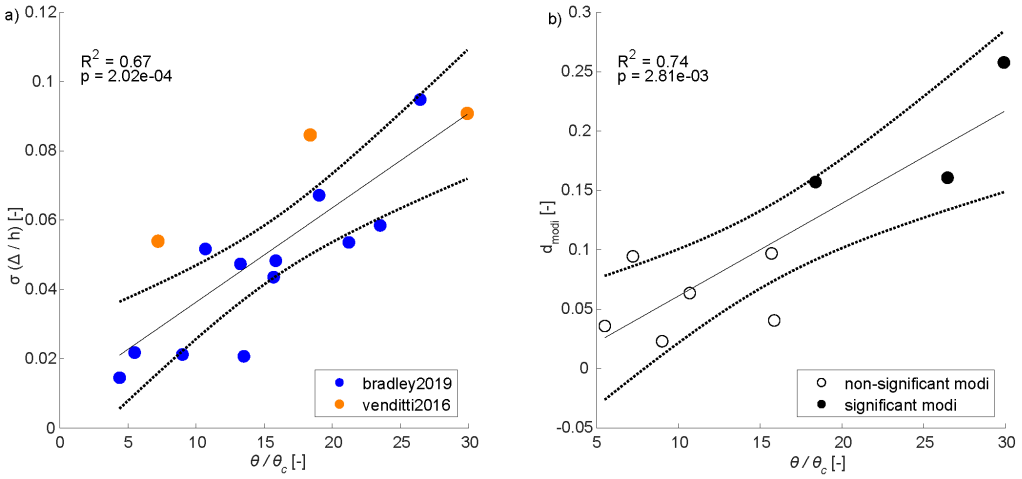

Figure 3. a) Standard deviation σ of the non-dimensional dune height Δ/h against transport stage θ/θ_c. b) The distributions of non-dimensional dune height are often bimodal, and the distance between the modi (d_{modi}) increases with increasing transport stage. Significant bimodal distributions ($d_{modi} >$ CV) are indicated with a filled marker; non-significant bimodality with an open marker.

different transport stages, the observed dune height distribution is significantly bimodal (Figure 3b).

For transport stages where dune heights are unimodally distributed, the parabolic dune height predictor (equation 1) is a good fit through these dune height modes. For transport stages where dune height is bimodally distributed (either with significant or non-significant bimodality), the dune height predictor is a good fit through the lowest modal value of of these bimodal distributions. For transport stages exceeding 18, the emergence of a statistically significant second mode at higher dune heights suggests a second equilibrium solution that branches off the parabolic dune height predictor, starting roughly at the top of the parabolic relation.

The pitchfork bifurcation (Figure 2) is no perfect model to fit to the observations. This bifurcation type shows a parabolic "central" solution that becomes unstable beyond the top of the parabola, and two diverging solutions branching off from there. Our observations, on the other hand, suggest that the parabolic solution itself remains stable for all transport stage values, but that a second solution branches off towards higher dune heights. Nonetheless, we consider the pitchfork bifurcation here, as it is the simplest mathematical model to illustrate how a second equilibrium can emerge beyond a tipping point (here: a critical transport stage), and how this may result in flickering between two states (Figure 1b,c) and bimodal dune height distributions with increasing spacing between modes (Figures 3, 4).

3.3 Physical explanation

We hypothesise that the changing states are a result of a temporary shift from suspended-dominated conditions to mixed- or bed load-dominated conditions. During bed load or mixed load conditions, there is a neutral or negative spatial lag between dune crest and maximum sediment transport rate, causing maintenance or growth of the dunes (Naqshband et al., 2017). During high flow conditions (suspended load dominated), a high concentration of sediment near the bed (Baas and Koning, 1995; Naqshband et al., 2014) causes the spatial lag to be positive, resulting in the washing out of dunes. Suspended load does not con-

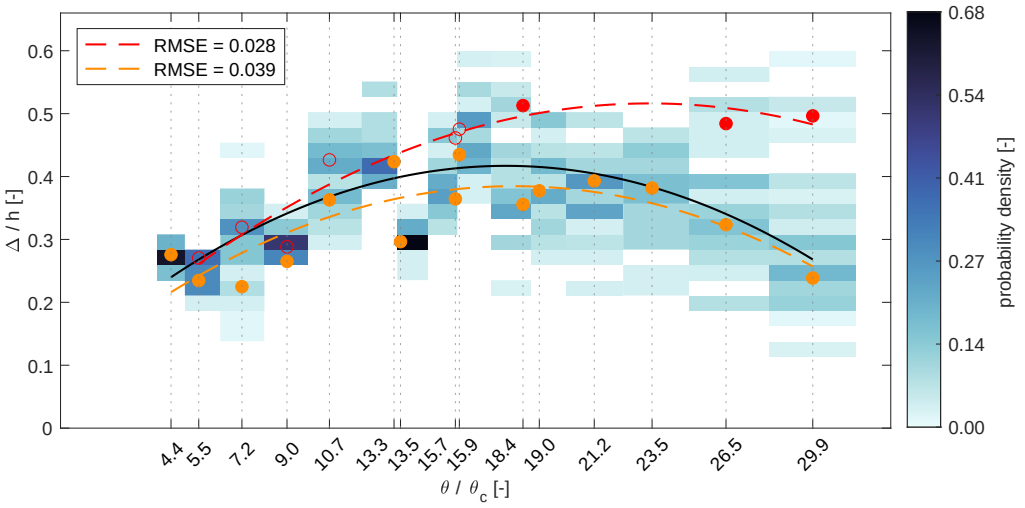

Figure 4. Density plot of the observations from Venditti et al. (2016) and Bradley and Venditti (2019), binned as a function of dune height Δ scaled by mean water depth h, and mean transport stage θ/θ_c. Mean values of transport stage are chosen since they are independent of the bed state. Orange bullets indicate the lower modal value found for that transport stage; red bullets indicate the higher modal value, if found for that transport stage. If the distribution for a specific transport stage is significantly bimodal, the red bullet marking the higher mode is filled; if non-significant, the red bullet is kept open. Quadratic relations were fitted through the orange bullets (orange dashed line) and through the red bullets (both filled and open; red dashed line). The black line indicates the dune height predictor (equation 1). Note that the vertical axis is divided into equidistant bins, while the transport stages along the horizontal axis are non-equidistant. Therefore, it was here assumed that, along the horizontal axis, each bin ranges until halfway between two subsequent transport stage values, which causes the bullets to not always be in the middle of the bins. For the left-most (right-most) transport stage value, the leftward (rightward) bin width is chosen the same as the rightward (leftward) bin width. Some tick labels along the horizontal axis are slightly displaced to avoid overlap, but ticks themselves are in the correct place.

tribute to the migration of dunes (neither in subaqueous (Naqshband et al., 2017) or aeolian conditions (Courrech du Pont, 2015)), but only to the deformation, causing a transition to plane bed (Naqshband et al., 2017; Naqshband and Hoitink, 2020). Washout conditions Best and Bridge (1992) found episodic short-lived outbursts of bed load sediment transport, that are also observed in aeolian transport (Livingstone et al., 2007; Butterfield, 1991; Baas and Sherman, 2005). A local outburst of sediment (local erosion, or local disruptive pulses) can result into local bed- or mixed load conditions. This can temporarily result in dune formation, until suspended load conditions dominate and the bed flattens out.

The temporary formation of dunes and flattening out again could be the cause for the observed flickering. This flickering can be seen as noise-induced tipping. Noise-induced tipping means that a system is perturbed by a forcing whose time-scale is shorter than the system's intrinsic time scale (Ashwin et al., 2012; Scheffer et al., 2009). Local bed load conditions can cause the noise that tips the system. With an increase in transport stage, the likelihood of those outbursts to actually result into local bed load transport decreases, and local outbursts are more likely to be transported as suspended load. This means that the magnitude of the noise (i.e. the intensity of the local bed load conditions) decreases with increasing transport stage. Since a decrease in the lower modi of dune height is observed with an increasing transport stage (if the transport stage is larger than 18), it can be recognized that the magnitude of the noise scales with the state of the system (dune height), a phenomenon that is more generally observed in flickering processes (Dakos et al., 2013). Practically, this means that the system might eventually become 'trapped' in the stable state that is Upper Stage Plane Bed, while the alternative state becomes abandoned. This theory needs to be tested, as to date it is unclear if a fully stable USPB exists.

The observed flickering behavior is not an artifact from the recirculating flume. Parker (2003) suggests that an artifact of recirculating flumes could be migrating lumps of sediment that persist for a long period of time until equilibrium is achieved. In the experiments of Venditti et al. (2016) and Bradley and Venditti (2019), a constant flow was applied until the bed reached equilibrium. Venditti et al. (2016) defined equilibrium conditions when no changes in the water depth and bed slope appeared anymore, which was after 72 hours for low transport stage runs, and after 30 hours for high transport stage runs. Bradley and Venditti (2019) allowed a constant flow of 10 to 25 hours depending on the transport stage until bedform height did not change anymore. Finally, Venditti et al. (2016) pointed out that one configuration is stable for a few minutes to half an hour. This indicates that there is no obvious regularity in the changes in bed configuration, which would be expected if this was due to migrating lumps in the recirculation system.

3.4 Implications

Flickering alternative stable bed morphological states at high transport stages has several implications. At higher flow stages, the bed may not necessarily get flatter (by an increase in dune length), but rapidly switch between bed configurations. This means that one single snapshot is not enough to capture the state of the system. Field monitoring with multi-beam measurements at high flow stages only provide a snapshot of the bed state, and accompanying logistical decisions (for e.g. high water protection, fairway depth, stability of buried pipes and cables) could not solely be based on this snapshot. At high flow conditions, many measurements in time are needed to get a complete appreciation of occurring bed states, and the large standard deviations here (Figure 1) indicate that mean values might be meaningless.

Laboratory experiments are known to be effective representations of the field, due to the natural scale independence of physical (geomorphological) processes (Paola et al., 2009). However, in scientific study designs, the repeatability of experiments should be considered. The presence of flickering behavior results in serious dependence of the results to the timing of the measurements. This means that studies should not only focus on

reproducibility (confirmation of the findings using different resources in an independent program), as suggested by Church et al. (2020), but also on repeatability (exact repetition of experiments to establish precision of results) of the experiments. When the temporal resolution of the measurements is less than the occurrence of flickering, there is a need for repetition of the experiments, because alternative bed states might not be detected. Geng et al. (2023) found that the development of a morphological system depends on the the initial bed conditions. The existence of multiple equilibria potentially increases the sensitivity to initial bed conditions, which once more stresses the need for repetition of experiments.

The classic equilibrium predictors might need to be revised to include this flickering behavior. Although Bradley and Venditti (2019) already suggests the need for averaging many values, and Venditti and Bradley (2022) binned observations to obtain the equation relating dune height to transport stage, it is questionable if the average dune height is a relevant parameter when a bimodal distribution is featured with high transport stages. The equilibrium predictor is based on empirical relations fitted through averaged data, and may not grasp the right physical processes.

Future research about the flickering behavior around the transition from dunes to USPB is critical, and longer high frequency time series of laboratory and field data should be acquired. A suggested next step could be detailed experimental observations of the critical transition over a longer (weeks) time scale. From this, the life time of the different phases could be determined (Arani et al., 2021), and a physical explanation for this phenomenon can be sought. This could be followed up by experiments using an increasing discharge over time, to observe the temporal changes in bed configuration and to confirm the type of tipping point.

4 Conclusion

We reanalyzed 15 laboratory experiments of bedform height over time from Venditti et al. (2016) and Bradley and Venditti (2019). The standard deviation and the bimodality of the datasets indicate flickering behavior at high transport stages:

- The standard deviation of bedform height over time increases with an increasing transport stage. The bed can rapidly switch between bed configurations. The quantified distributions of bedform height show increasingly strong signs of bimodality. The distance between the two modi increases with increasing transport stage, and bimodality is significant for transport stages exceeding 18.
- The modi in the dune height distributions feature two branches. The lowest modi represents the branch that is also captured by the dune geometry predictor of Venditti and Bradley (2022). The other branch, that indicates the presence of large dunes at high transport stages, is not captured by the predictor.
- This behavior is an indication that a second equilibrium state emerges for transport stages beyond approximately 18. Above this tipping point, repeated critical transitions triggered by stochastic perturbations (flickering) between the two alternative states results in the bimodal distribution as observed in the experiments.
- We hypothesise that this is the result of local outbursts of bedload sediment, resulting in a localized bedload transport, enabling dune growth. The likelihood that these outbursts actually result in local bedload conditions decreases with increasing transport stage, and decreasing averaged dune height. Therefore, the system eventually gets trapped in the Upper Stage Plane Bed-state, where perturbations are not strong enough to tip the system to the alternative state.
- The existence of flickering of a sediment bed has far-reaching consequences for field measurements, laboratory experimental design, and calls for reinterpretation of the classical equilibrium relations.

Open Research Section

Data is available through Venditti et al. (2016) and Bradley and Venditti (2019). The code used to generate the results in this study will be made available through the public repository of 4TU upon acceptance.

Acknowledgments

SIdL, RCvdV and AJFH were funded by the Netherlands Organisation for Scientific Research (NWO), within Vici project "Deltas out of shape: regime changes of sediment dynamics in tide-influenced deltas" (Grant NWO-TTW 17062).

References

Amsler, M.L. and M.H. Garcia (1997). "Sand-dune geometry of large rivers during floods". In: *Journal of Hydraulic Engineering* 123.6.

Amsler, M.L. and M.I. Schreider (1999). "Dune height prediction at floods in the Paraná River, Argentina". In: *River sedimentation: Theory and applications*, pp. 615–620.

Arani, Babak M.S. et al. (2021). "Exit time as a measure of ecological resilience". In: *Science* 372.6547. ISSN: 10959203. DOI: 10.1126/science.aay4895.

ASCE Task Force (2002). "Flow and transport over dunes". In: *Journal of Hydraulic Engineering* 127, pp. 726–728.

Ashwin, Peter et al. (2012). "Tipping points in open systems: bifurcation, noise-induced and rate-dependent examples in the climate system". In: *Philosophical Transactions of the Royal Society A: Mathematical, Physical and Engineering Sciences* 370.1962, pp. 1166–1184. ISSN: 1364-503X. DOI: 10.1098/rsta.2011.0306.

Baas, A. C. W. and D. J. Sherman (2005). "Formation and behavior of aeolian streamers". In: *Journal of Geophysical Research: Earth Surface* 110.F3. ISSN: 0148-0227. DOI: 10.1029/2004JF000270.

Baas, J.H. and H. de Koning (1995). "Washed-Out Ripples: Their Equilibrium Dimensions, Migration Rate, and Relation to Suspended-Sediment Concentration in Very Fine Sand". In: *SEPM Journal of Sedimentary Research* Vol. 65A. ISSN: 1527-1404. DOI: 10.1306/D42680E5-2B26-11D7-8648000102C1865D.

Berg, J.H. van den and A. van Gelder (1993). "A new bedform stability diagram, with emphasis on the transiton of ripples to plane bed in flows over fine sand and silt". In: *Spec. Publs Int. Ass. Sediment* 17, pp. 11–21.

Best, Jim (2005). "The fluid dynamics of river dunes: A review and some future research directions". In: *Journal of Geophysical Research: Earth Surface* 110.4, pp. 1–21. ISSN: 21699011. DOI: 10.1029/2004JF000218.

Best, Jim and John Bridge (1992). "The morphology and dynamics of low amplitude bedwaves upon upper stage plane beds and the preservation of planar laminae". In: *Sedimentology* 39.5, pp. 737–752. ISSN: 13653091. DOI: 10.1111/j.1365-3091.1992.tb02150.x.

Bradley, Ryan W. and Jeremy G. Venditti (2017). *Reevaluating dune scaling relations*. DOI: 10.1016/j.earscirev.2016.11.004.

— (2019). "Transport Scaling of Dune Dimensions in Shallow Flows". In: *Journal of Geophysical Research: Earth Surface* 124.2, pp. 526–547. ISSN: 21699011. DOI: 10.1029/2018JF004832.

Butterfield, G. R. (1991). "Grain transport rates in steady and unsteady turbulent airflows". In: pp. 97–122. DOI: 10.1007/978-3-7091-6706-9{_}6.

Carpenter, S. R. and W. A. Brock (2006). "Rising variance: a leading indicator of ecological transition". In: *Ecology Letters* 9.3, pp. 311–318. ISSN: 1461023X. DOI: 10.1111/j.1461-0248.2005.00877.x.

Church, M. et al. (2020). "Are Results in Geomorphology Reproducible?" In: *Journal of Geophysical Research: Earth Surface* 125.8. ISSN: 2169-9003. DOI: 10.1029/2020JF005553.

Courrech du Pont, Sylvain (2015). "Dune morphodynamics". In: *Comptes Rendus Physique* 16.1, pp. 118–138. ISSN: 16310705. DOI: 10.1016/j.crhy.2015.02.002.

Dakos, Vasilis, Egbert H. van Nes, and Marten Scheffer (2013). "Flickering as an early warning signal". In: *Theoretical Ecology* 6.3, pp. 309–317. ISSN: 18741738. DOI: 10.1007/s12080-013-0186-4.

Dakos, Vasilis et al. (2012). "Methods for detecting early warnings of critical transitions in time series illustrated using simulated ecological data". In: *PLoS ONE* 7.7. ISSN: 19326203. DOI: 10.1371/journal.pone.0041010.

Geng, L. et al. (2023). "The Sensitivity of Tidal Channel Systems to Initial Bed Conditions, Vegetation, and Tidal Asymmetry". In: *Journal of Geophysical Research: Earth Surface* 128.3. ISSN: 2169-9003. DOI: 10.1029/2022JF006929.

Gilbert, G.K. (1914). "The transport of debris by running water". In: *USGS Professional Paper* 86, pp. 1–263.

Greene, H. Gary, Matthew Baker, and John Aschoff (2020). "A dynamic bedforms habitat for the forage fish Pacific sand lance, San Juan Islands, WA, United States". In: *Seafloor Geomorphology as Benthic Habitat*. Elsevier, pp. 267–279. DOI: 10.1016/B978-0-12-814960-7.00014-2.

Guy, H.P., D.B. Simons, and E.V. Richardson (1966). "Summary of alluvial channel data from flume experiments, 1956–1961." In: *USGS Professional Paper 462-I, 1–96.*, pp. 1–96.

Hoitink, A. J. F. et al. (2020). "Resilience of River Deltas in the Anthropocene". In: *Journal of Geophysical Research: Earth Surface* 125.3. ISSN: 2169-9003. DOI: 10.1029/2019JF005201.

Horsthemke, W. and R. Lefever (1984). *Noise-induced transitions: Theory and applications in physics, chemistry and biology*. 1. Springer. DOI: 10.1007/BF00047115.

Julien, P.Y. and G.J. Klaassen (1995). "Sand-dune geometry of large rivers during floods". In: 121.9, pp. 657–663.

Karim, F. (1995). "Bed configuration and hydraulic resistance in alluvial-channel flows". In: *Journal of Hydraulic Engineering* 121.1, pp. 15–25.

Lenton, Timothy M. (2013). "Environmental Tipping Points". In: *Annual Review of Environment and Resources* 38.1, pp. 1–29. ISSN: 1543-5938. DOI: 10.1146/annurev-environ-102511-084654.

Livingstone, Ian, Giles F.S. Wiggs, and Corinne M. Weaver (2007). "Geomorphology of desert sand dunes: A review of recent progress". In: *Earth-Science Reviews* 80.3-4, pp. 239–257. ISSN: 00128252. DOI: 10.1016/j.earscirev.2006.09.004.

Naqshband, S. and A. J. F. Hoitink (2020). "Scale-Dependent Evanescence of River Dunes During Discharge Extremes". In: *Geophysical Research Letters* 47.6. ISSN: 0094-8276. DOI: 10.1029/2019GL085902.

Naqshband, S., J.S. Ribberink, and S.J.M.H. Hulscher (2014). "Using both free surface effect and sediment transport mode parameters in defining the morphology of river dunes and their evolution to upper stage plane beds". In: *Journal of Hydraulic Engineering* 140.6, pp. 1–6. ISSN: 19437900. DOI: 10.1061/(ASCE)HY.1943-7900.0000873.

Naqshband, S. et al. (2017). "A Sharp View on River Dune Transition to Upper Stage Plane Bed". In: *Geophysical Research Letters* 44.22, pp. 437–11. ISSN: 19448007. DOI: 10.1002/2017GL075906.

Paola, Chris et al. (2009). "The "unreasonable effectiveness" of stratigraphic and geomorphic experiments". In: *Earth-Science Reviews* 97.1-4, pp. 1–43. ISSN: 00128252. DOI: 10.1016/j.earscirev.2009.05.003.

Parker, Gary (2003). "Persistence of sediment lumps in approach to equilibrium in sediment-recirculating flumes". In: *Proceedings, International Association of Hydraulic Research Congress*.

Saunderson, Houston C and Francis P J Lockett (1983). "Flume experiments on bedforms and structures at the dune-plane bed transition". In: *Spec Publs. int. Ass Sediment* 6, pp. 49–58.

Scheffer, Marten et al. (2009). *Early-warning signals for critical transitions*. DOI: 10.1038/nature08227.

Scheffer, Marten et al. (2012). "Anticipating Critical Transitions". In: URL: https://www.science.org.

Southard, John B and Lawrence A Boguchwal (1990). "Bed configurations in steady unidirectional water flows, part 2. Synthsis of flume data." In: 60.5, pp. 658–679.

Statisticat, L.L.C. (2021). *LaplacesDemon: Complete Environment for Bayesian Inference*. URL: https://web.archive.org/web/20150206004624/http://www.bayesian-inference.com/software.

Strogatz, Steven H. (2018). *Nonlinear Dynamics and Chaos with Student Solutions Manual*. CRC Press. ISBN: 9780429399640. DOI: 10.1201/9780429399640.

Venditti, Jeremy G. and Ryan W. Bradley (2022). "Bedforms in Sand Bed Rivers". In: *Treatise on Geomorphology*. Elsevier, pp. 222–254. ISBN: 9780128182352. DOI: 10.1016/B978-0-12-409548-9.12519-9.

Venditti, Jeremy G., C. Y.Martin Lin, and Moslem Kazemi (2016). "Variability in bedform morphology and kinematics with transport stage". In: *Sedimentology* 63.4, pp. 1017–1040. ISSN: 13653091. DOI: 10.1111/sed.12247.

Warmink, J. J. et al. (2013). "Quantification of uncertainty in design water levels due to uncertain bed form roughness in the Dutch river Waal". In: *Hydrological Processes* 27.11, pp. 1646–1663. ISSN: 08856087. DOI: 10.1002/hyp.9319.